Available online at www.sciencedirect.com

ScienceDirect

Developmental Biology 299 (2006) 105–121

DEVELOPMENTAL BIOLOGY

www.elsevier.com/locate/ydbio

Major sperm protein signaling promotes oocyte microtubule reorganization prior to fertilization in *Caenorhabditis elegans*

Jana E. Harris [1], J. Amaranath Govindan [1,2], Ikuko Yamamoto, Joel Schwartz [3], Irina Kaverina, David Greenstein [*,2]

Department of Cell and Developmental Biology, Vanderbilt University School of Medicine, 465 21st Avenue South, Nashville, TN 37232, USA

Received for publication 2 June 2006; revised 10 July 2006; accepted 11 July 2006
Available online 15 July 2006

Abstract

In most animals, female meiotic spindles assemble in the absence of centrosomes; instead, microtubule nucleation by chromatin, motor activity, and microtubule dynamics drive the self-organization of a bipolar meiotic spindle. Meiotic spindle assembly commences when microtubules gain access to chromatin after nuclear envelope breakdown (NEBD) during meiotic maturation. Although many studies have addressed the chromatin-based mechanism of female meiotic spindle assembly, it is less clear how signaling influences microtubule localization and dynamics prior to NEBD. Here we analyze microtubule behavior in *Caenorhabditis elegans* oocytes at early stages of the meiotic maturation process using confocal microscopy and live-cell imaging. In *C. elegans*, sperm trigger oocyte meiotic maturation and ovulation using the major sperm protein (MSP) as an extracellular signaling molecule. We show that MSP signaling reorganizes oocyte microtubules prior to NEBD and fertilization by affecting their localization and dynamics. We present evidence that MSP signaling reorganizes oocyte microtubules through a signaling network involving antagonistic $G\alpha_{o/i}$ and $G\alpha_s$ pathways and gap-junctional communication with somatic cells of the gonad. We propose that MSP-dependent microtubule reorganization promotes meiotic spindle assembly by facilitating the search and capture of microtubules by meiotic chromatin following NEBD.

Keywords: Meiosis; Microtubule; Oocyte; Meiotic maturation; Signaling; *C. elegans*; Somatic gonad; G-protein

Introduction

Meiosis generates haploid gametes, which combine through fertilization to generate a diploid zygote (reviewed by Page and Hawley, 2004). The viability of the resulting embryo, and the whole species for that matter, depend critically on the faithful segregation of the genetic material during meiosis. Nondisjunction during either of the meiotic divisions gives rise to aneuploid embryos, containing too many or too few chromosomes, typically with dire consequences owing to the deleterious effects of abnormal gene dosage. In humans, nondisjunction during female meiosis I represents the leading cause of miscarriage and congenital birth defects, such as Down syndrome (Hassold and Hunt, 2001). Previous studies in humans and mice suggest that disturbances in the hormonal regulation of folliculogenesis are associated with chromosome congression failure during meiotic spindle assembly and may represent a significant risk factor for nondisjunction errors (Hodges et al., 2002). At present, it is not understood how signals that regulate oocyte growth and meiotic progression might influence meiotic spindle assembly and chromosome segregation.

The meiotic spindles of most animal oocytes are distinctive from mitotic spindles of somatic cells in terms of their mechanism of assembly, their function, and their modes of regulation. The female meiotic spindles of many species are both acentriolar and anastral (Albertson and Thomson, 1993; Matthies et al., 1996; Schatten, 1994; Szollosi et al., 1972). Instead of relying on centrosomes, which are eliminated during oogenesis in many species, the meiotic chromatin directs

* Corresponding author. Fax: +1 612 626 6140.
E-mail address: green959@umn.edu (D. Greenstein).
[1] These authors made equal contributions to this work.
[2] Present address: Department of Genetics, Cell Biology, and Development, University of Minnesota, Minneapolis, MN 55455, USA.
[3] Present address: Stowers Institute, 1000 E. 50th St., Kansas City, MO 64110, USA.

0012-1606/$ - see front matter © 2006 Elsevier Inc. All rights reserved.
doi:10.1016/j.ydbio.2006.07.013

assembly of a bipolar spindle both by nucleating microtubules and organizing preexisting microtubules, which then self-organize through incompletely understood mechanisms involving microtubule motors and dynamics (Heald et al., 1996; Matthies et al., 1996; Skold et al., 2005; Walczak et al., 1998). Biochemical studies in *Xenopus* egg extracts, which

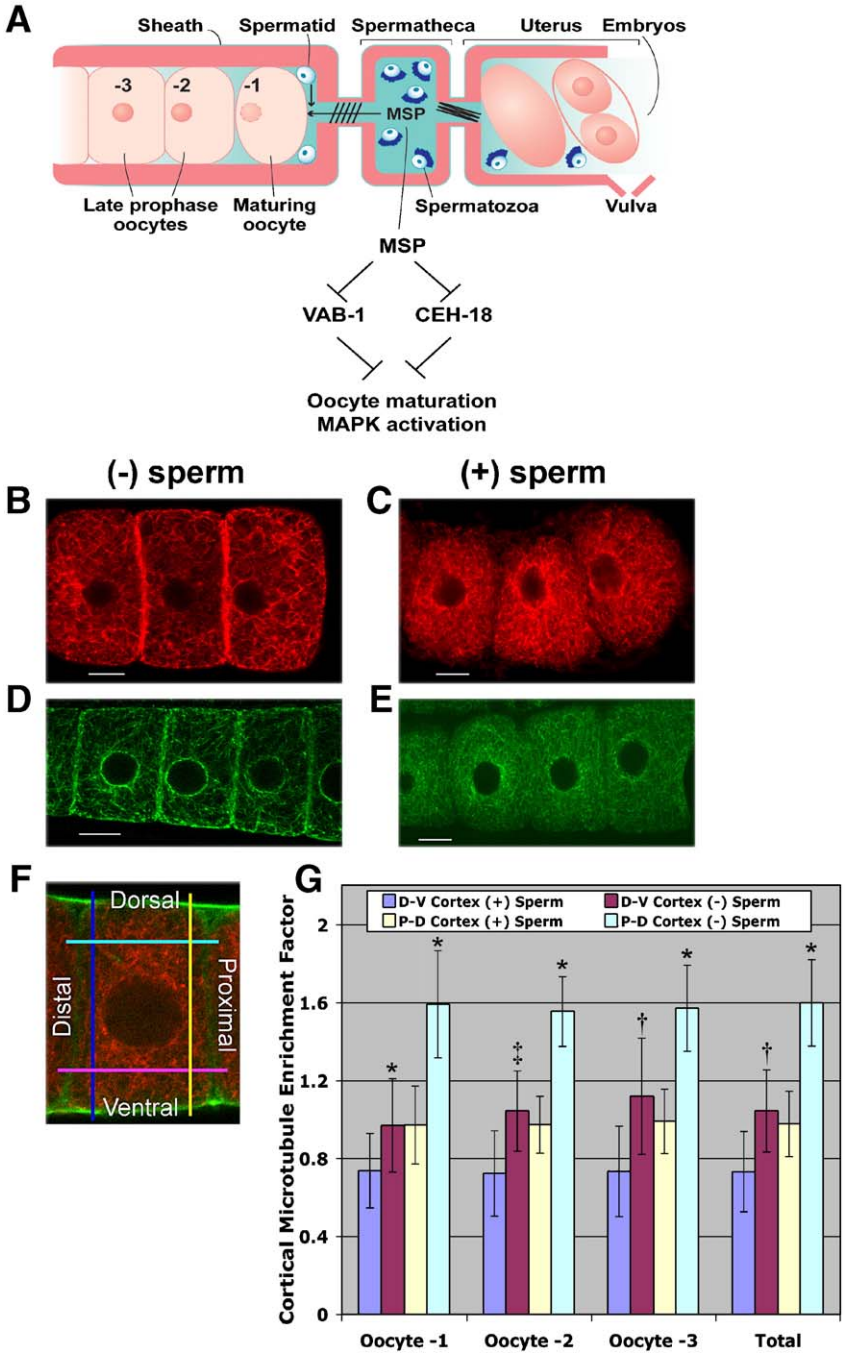

Fig. 1. Organization of microtubules in *C. elegans* oocytes. (A) Diagram of the hermaphrodite reproductive tract. Oocytes undergo meiotic maturation in an assembly-line fashion in response to the extracellular MSP signal (depicted in light blue), which exhibits a graded distribution from proximal to distal in mated females. MSP functions by antagonizing the VAB-1 and CEH-18 pathways to promote meiotic maturation. In all depictions and photomicrographs of the gonad, proximal is at the right, and distal is at the left. The −1 through −3 oocytes are indicated. (B–E) Single confocal images of the oocyte microtubule cytoskeleton in dissected and fixed gonads (B and C) or living animals (D and E) showing the localization of α-tubulin (B and C) or β-tubulin::GFP (D and E). (B and D) In unmated females, microtubules are cortically enriched between oocytes. (C and E) Microtubules are evenly dispersed throughout the cytoplasm in the most proximal oocytes in mated *fog-2(q71)* females. The perinuclear accumulation of microtubules observed in panel D and in subsequent figures is variable. (F) Single confocal image of a proximal oocyte in a dissected gonad stained for α-tubulin (red) and actin (green), illustrating the strategy for quantifying microtubule enrichment along the proximal–distal and dorsal–ventral axes with representative line scans drawn using Metamorph software. (G) Comparison of cortical microtubule enrichment factors from unmated and mated females at the proximal–distal and dorsal–ventral cortices of the −1 through −3 oocytes (in this and subsequent bar graphs the −1 oocyte is on the left). *t* test between mated and unmated females, $*p<0.0001$, $^{\dagger}p<0.01$, or $^{\ddagger}p<0.05$, error bars represent SD. Scale bars: 10 μm.

provide a model for assembly of the meiosis II spindle, indicate that DNA-coated beads can drive the self-organization of microtubules into bipolar spindles (Heald et al., 1996). Cultured mammalian cells might utilize analogous mechanisms in parallel with centrosome-dependent mechanisms as bipolar spindles can assemble after laser ablation of centrosomes (Khodjakov et al., 2000). Chromatin-based microtubule assembly pathways employ Ran-GTP-dependent mechanisms (Carazo-Salas et al., 1999; Kalab et al., 1999; Ohba et al., 1999; Wilde and Zheng, 1999), as well as mechanisms utilizing the Aurora B kinase chromosomal passenger complex (Sampath et al., 2004).

Assembly of a bipolar meiotic spindle requires that the cytoplasmic microtubules gain access to the nuclear environment, which occurs upon nuclear envelope breakdown (NEBD) during the meiotic maturation process. Although there have been many biochemical and cell biological investigations of meiotic spindle assembly, few studies have examined microtubule behavior during the earliest stages before cytoplasmic microtubules become associated with chromatin upon NEBD. Studies in sea urchin oocytes have revealed that cortical microtubules undergo a dramatic structural reorganization from an extensive basket-like array to a diminishing population of shorter microtubules during meiotic maturation (Boyle and Ernst, 1989). The signaling mechanisms that bring about these major cytoplasmic changes and their potential biological significance are, however, unclear. In this study, we address how meiotic maturation signaling influences microtubule localization and dynamics prior to NEBD in the nematode *Caenorhabditis elegans*.

C. elegans is an ideal system for studying the effects of hormonal signaling on oocyte microtubules during the meiotic maturation process. These animals are transparent so meiotic maturation can be directly observed (McCarter et al., 1999; Ward and Carrel, 1979), and recent studies have begun to elucidate the key intercellular signaling pathways that regulate this process (reviewed by Yamamoto et al., 2006). In *C. elegans*, sperm trigger oocyte meiotic maturation using the major sperm protein (MSP) as a signaling molecule (Miller et al., 2001, 2003; Kosinski et al., 2005; Govindan et al., 2006). MSP is also the key cytoskeletal element required for the actin-independent amoeboid locomotion of nematode spermatozoa (Bottino et al., 2002; Italiano et al., 1996). Because hermaphrodites produce only a fixed number of sperm, meiotic maturation rates are initially high, but decline as sperm are consumed by fertilization and levels of the MSP signal decline (McCarter et al., 1999; Kosinski et al., 2005). In sex-determination mutants of *C. elegans* that feminize the gonad (e.g., *fog-2* or *fog-3*) such that no sperm are produced, oocytes arrest at the diakinesis stage until sperm are supplied by mating.

In *C. elegans*, meiotic maturation and ovulation are coupled to sperm availability through a complex regulatory network involving germline and somatic controls (Corrigan et al., 2005; Miller et al., 2003). Parallel genetic pathways defined by *vab-1*, which encodes an MSP-binding ephrin receptor, and *ceh-18*, which encodes a POU-homeoprotein expressed in gonadal sheath cells but not oocytes, together compose an MSP-sensing control mechanism that regulates meiotic maturation (Fig. 1A; Miller et al., 2003; Govindan et al., 2006). Somatic control of meiotic maturation, likely through the *ceh-18* pathway, involves antagonistic $G\alpha_{o/i}$ and $G\alpha_s$ signaling pathways that define negatively- and positively-acting inputs, respectively (Govindan et al., 2006). $G\alpha_s$ signaling is necessary and sufficient to trigger oocyte mitogen-activated protein kinase (MAPK) activation and meiotic maturation, in part, through antagonizing inhibitory sheath/oocyte gap-junctional communication. Although these studies provided initial insights into the complex signaling pathways regulating meiotic maturation in response to MSP in *C. elegans*, they raise new questions about how the *vab-1* and *ceh-18* pathways control nuclear and cytoplasmic events during maturation, as well as the division of labor among the pathways. Here, we provide evidence that MSP signaling reorganizes the microtubule cytoskeleton of oocytes prior to NEBD. Using laser-scanning and spinning-disk confocal microscopy, we found that cortical microtubule localization and plus-end dynamics are altered in the presence of the MSP signal. The VAB-1 Eph/MSP receptor pathway has no apparent role in regulating the distribution of oocyte microtubules. By contrast, the somatic *ceh-18* pathway involving antagonistic $G\alpha_{o/i}$ and $G\alpha_s$ signaling influences the microtubule cytoskeleton of the oocyte. We propose a model in which MSP signaling alters microtubule localization and plus-end dynamics to facilitate the search and capture of microtubules by chromatin during meiotic spindle assembly.

Materials and methods

Nematode strains, nomenclature, and phenotypic analysis

Standard techniques were used for nematode culture at 20°C, except where indicated otherwise. The *C. elegans var. Bristol* strain, N2, was used as the wild-type hermaphrodite strain. We used *fog-2(q71)* and *fog-3(q443)* mutations, which feminize the germ line, to generate *XX* animals that do not produce sperm (females), a situation we refer to as a "minus sperm" condition to simplify the flow of information. Similarly, the "plus sperm" condition refers to experiments using either mated females or hermaphrodites as indicated. In all tested cases, mutations in *fog-2* and *fog-3* gave identical results and thus could be used interchangeably; however, for technical reasons most experiments were performed using *fog-2(q71)*, unless genetic markers on *LGI* were utilized. Key strains and alleles used are described in WormBase (http://www.wormbase.org), in Govindan et al. (2006), or as follows:

LGI: *gsa-1(ce81)*, *gsa-1(ce94)*, *goa-1(sa734)*, *rrf-1(pk1417)*, *fog-3(q443)*
LGII: *vab-1(dx31)*, *ptc-1(ok122)*
LGIII: *mpk-1(ga111ts)*, *cgh-1(ok492)*
LGIV: *unc-24(e138)*, *oma-1(zu40te33)*, *fem-3(e1990)*
LGV: *oma-2(te51)*, *emo-1(oz1)*, *fog-2(q71)*
LGX: *ceh-18(mg57)*, and *kin-2(ce179)*.

Rearrangements used were *hT2(qIs48)(I, III)*, *mIn1II*, and *DnT1(IV, V)*. Transgenes used were TH66 *pie-1∷ebp-2∷gfp* (Srayko et al., 2005) and AZ244 *pie-1∷gfp∷tubulin* (Praitis et al., 2001).

RNA interference employed a modification of the method of Kamath and Ahringer (2003), which was performed as described (Govindan et al., 2006). MSP injections (200 nM MSP-142) and analysis of oocyte MAPK activation were described in Miller et al. (2001). To reduce the extent of MAPK activation, *fog-2(q71)* females were microinjected with the MEK1/2 inhibitor, U0126 (100 μM in egg salts; Sigma). cAMP-soaking experiments utilized an 8 mg/ml dibutyryl cyclic AMP (Sigma) in M9 buffer.

Fluorescence microscopy

Preparation of dissected gonads and antibody staining

Gonads were dissected, fixed, and stained for immunofluorescence microscopy as described (Rose et al., 1997). GFP fluorescence was analyzed in whole-mount using 0.1% tricaine/0.01% tetramisole treatment for 30 min as an anesthetic (McCarter et al., 1999) or in unfixed dissected gonads, which were mounted on agar pads using double-sided tape as a spacer to prevent the cover glass from smashing the gonads. Antibodies used were YL1/2 rat monoclonal anti-α-tubulin (Kilmartin et al., 1982) (Accurate Chemical and Scientific Corporation); mouse monoclonal anti-actin (MP Biomedicals); anti-CeGrip-1 (kindly provided by Karen Oegema and Tony Hyman); anti-MAPK-YT (Sigma); and Cy2- or Cy3-conjugated secondary antibodies (Jackson ImmunoResearch Laboratories).

Laser-scanning confocal microscopy

Confocal images were acquired on a Zeiss LSM510 microscope with a pinhole of 1.0 Airy Units and 63× (NA 1.4) objective lens. Gain and offset were set so that all data were within the dynamic range of the PMT. Band-pass filters were used to optically isolate the Cy2 and Cy3 fluorophores, and no cross-talk was observed.

Quantitation of cortical microtubule enrichment

To calculate the cortical microtubule enrichment factor (CMEF), *z*-stack images of dissected gonads labeled with anti-tubulin and anti-actin antibodies were obtained on the confocal microscope and analyzed using MetaMorph software (Universal Imaging). Cross-sectional images through medial focal planes were analyzed to avoid the overlying gonadal sheath cells. For each oocyte analyzed, ten line scans, each 10 pixels thick, were drawn from either the proximal to distal cortex or from the dorsal to ventral cortex, avoiding the nucleus. For each pixel, the corresponding intensities for tubulin and actin were then exported into an Excel spreadsheet (Microsoft). The cortex was defined operationally, using an observer blind method, as the region of the micrograph in which the actin intensity was greater than one standard deviation above its mean. Use of line scans, instead of regions of interest, reduced the potential for sampling bias; however, the use of a mathematical definition of the cortex tended to reduce the magnitude of the increase in cortical enrichment in females. The CMEF was defined as the ratio of the average microtubule intensity at the cortex to the average microtubule intensity in the cytoplasm. Use of a ratio enabled comparisons between separate experiments that may have had varying overall staining levels. Because we measured pixel intensities, we could exclude the possibility that our results were due to over-sampling cortical regions of adjacent oocytes relative to the cytoplasm. In time course analyses, CMEF values among oocytes −1 to −5 within each day examined, and among days examined within each oocyte, were tested using Fisher's protected least significant difference (*lsd*) method at $p=0.01$.

Spinning disk confocal microscopy

Spinning disk confocal microscopy used a Perkin Elmer Ultraview LCI system on a Zeiss 200M inverted microscope with a 63× (1.4 NA) objective lens. Images were acquired using an ORCA ER camera (Hamamatsu Photonics) and Ultraview software (Perkin Elmer). The thickness of the sample and the small size of the EBP-2∷GFP foci, coupled with the inherent photosensitivity of the meiotic maturation process (McCarter et al., 1999), represented technical difficulties. We were able to increase the signal-to-noise by utilizing a preparation in which the worm was decapitated to allow buffer exchange with the pseudocoelom or the gonad arm outside the carcass. Movies were obtained over 1 min in a single confocal plane (~0.4 μm thick) with a gain of 255, 1×1 binning, and an exposure of 250 ms. Images were acquired as a stream with no recovery time between images. The density of growing plus ends was measured in different regions of the oocyte by counting the number of brightly labeled EBP-2∷GFP foci in a 36.4-μm^3 region using Metamorph software. The directional movement of growing plus ends that remained in the focal plane for 3–5 consecutive frames was analyzed for 200 EBP∷GFP foci in each region of the oocyte using LSM Examiner (Zeiss) software. To calculate the rate of movement, we measured the distance a plus end traveled over 5 frames (~1.5 s) using Metamorph. Recordings and measurements were made in the −1 and −2 oocytes prior to NEBD and similar results were obtained.

Fluorescence recovery after photobleaching (FRAP)

FRAP was conducted on the LSM510 confocal microscope on a single confocal slice. A box of 77×24 pixels (73.92 μm^2) was bleached with 100% laser power after three pre-bleach images and fluorescence recovery was measured every 1.57 s over 77 images. Fluorescence recovery was observed in the cytoplasm and at the cortex of anesthetized *pie-1∷gfp∷tubulin* mated and unmated females (15 laser-pulse iterations per bleach) and *pie-1∷gfp* hermaphrodites and females (100 laser-pulse iterations per bleach). More laser-pulse iterations were needed to bleach GFP fluorescence in the *pie-1∷gfp* animals due to the greater GFP signal in oocytes. Fluorescence intensities within the bleached area of the cell were normalized to the intensities of the whole cell after correcting for the background fluorescence. FRAP experiments and measurements were made in the −1 and −2 oocytes prior to NEBD and similar results were obtained.

Results

MSP signals oocyte microtubule reorganization

Sperm dependence of microtubule reorganization

During female meiosis, dynamic microtubules assemble around chromatin instead of relying upon centrosomal microtubule-organizing centers (Varmark, 2004). Meiotic spindle assembly commences when the cytoplasmic microtubules gain access to the chromatin upon nuclear envelope breakdown (NEBD) during the oocyte meiotic maturation process. To investigate the origins of this specialized microtubule behavior during *C. elegans* oocyte meiotic maturation, we examined the organization of the dynamic microtubule cytoskeleton in oocytes prior to the onset of NEBD in the absence and presence of the MSP meiotic maturation signal. Because tyrosinated α-tubulin is associated with newly formed microtubule populations (Westermann and Weber, 2003), we used YL1/2 monoclonal antibodies to stain tyrosinated-α-tubulin in dissected and fixed gonads from unmated and mated *fog-2(q71)* females, and we analyzed the results using laser-scanning confocal microscopy (Figs. 1B and C). In unmated females, in which sperm are absent, microtubules are highly enriched at the proximal and distal cortical edges of oocytes but are sparsely dispersed throughout the cytoplasm (Fig. 1B). By contrast, in mated females, in which sperm are present, microtubules in proximal oocytes (−1 to −4) are evenly dispersed throughout the oocyte cytoplasm in a dense net-like array (Fig. 1C). Strikingly, the cortical enrichment of microtubules observed in the absence of sperm (Fig. 1B) is not observed in presence of sperm (Fig. 1C). This result suggests that the presence of sperm in the reproductive tract influences the organization of the oocyte microtubule cytoskeleton. Moreover, these data indicate that the sperm-dependent change in microtubule organization occurs prior to both NEBD, which is spatially restricted to the most proximal (−1) oocyte, and to fertilization, which occurs as the oocyte enters the spermatheca during ovulation (Fig. 1A).

To determine whether the detection of tyrosinated α-tubulin in dissected and fixed gonads reflects the localization of bulk microtubules in living animals, we compared oocyte microtubules in unmated and mated *fog-2(q71)* females containing a β-tubulin-GFP fusion using confocal microscopy (Figs. 1D and E). Using this method, we observed a similar difference between the microtubule organization of unmated and mated

females, with oocytes exhibiting an enrichment of microtubules at the proximal and distal cell cortex in the absence of sperm (Fig. 1D).

Measurement of cortical microtubule enrichment

To quantify this sperm-dependent difference in microtubule organization, we measured the average pixel intensity of cortical and cytoplasmic microtubules of the three most proximal oocytes in unmated ($n=25$) and mated ($n=34$) females and calculated a cortical microtubule-enrichment factor (CMEF), expressed as the ratio of cortical to cytoplasmic intensities (Figs. 1F and G; see Materials and methods). In the absence of sperm, we observed a significant ($p<0.0001$) 1.5-fold enrichment of microtubules at the proximal and distal cortices (CMEF = 1.51 ± 0.20). By contrast, microtubules were uniformly distributed throughout the cytoplasm of oocytes and were not enriched at the proximal and distal cortices of the cell in the presence of sperm (CMEF = 1.02 ± 0.20) (Fig. 1G). In the absence of sperm, microtubule enrichment is limited to the proximal and distal cortical edges between oocytes as demonstrated by the lack of comparable microtubule enrichment at the dorsal and ventral cortical edges of oocytes in females (CMEF = 1.04 ± 0.21, $n=30$) (Fig. 1G). In addition, microtubules were not highly enriched at the most proximal edge of the −1 oocyte, closest to the spermatheca, in females (CMEF = 1.12 ± 0.32, $n=10$) compared to the distal edge adjacent to the −2 oocyte (CMEF = 1.67 ± 0.29, $n=10$). These results define a sperm-dependent process, we term "oocyte microtubule reorganization," referring to the global transition between cortically enriched microtubules, as observed in unmated female oocytes, and uniformly distributed microtubules, as observed in oocytes from mated females.

Spatial and temporal distribution of cortical microtubule enrichment in hermaphrodites

C. elegans hermaphrodites produce a fixed amount of sperm. Consequently, extracellular levels of MSP in the reproductive tract and meiotic maturation rates progressively decline when sperm become depleted as hermaphrodites age (Kosinski et al., 2005). To determine whether microtubule reorganization is influenced by the decline in sperm numbers that occur as hermaphrodites age, we performed a time course analysis of microtubule organization in proximal oocytes (Figs. 2A–C). We found that CMEF values along the proximal–distal axis progressively increase over the first five days of adulthood from 0.95 ± 0.08 at day 1 ($n=76$) to 1.40 ± 0.04 at day 5 ($n=62$) (Fig. 2B), approaching the CMEF levels seen in unmated females (Fig. 1G). To distinguish between aging and the presence of sperm as factors promoting microtubule reorganization in hermaphrodites, we mated 4-day-old hermaphrodites and analyzed their microtubules on day 5. These mated old hermaphrodites displayed reorganized microtubules characteristic of young hermaphrodites (CMEF = 1.03 ± 0.23, $n=73$), suggesting that the presence of sperm, not age, is the key factor controlling microtubule organization in oocytes (Fig. 2B). Because the CMEF measurements in this time course analysis represent quantitative parameters describing oocyte microtubule organization, we applied the least significant difference (*lsd*) approach for performing pairwise comparisons to statistically analyze the CMEF values (see Materials and methods). This analysis indicates that microtubule reorganization is not an all-or-none phenomenon in that there is a temporally graded response with intermediate CMEF levels observed in oocytes from 2- to 3-day-old hermaphrodites (Figs. 2A and C). If MSP signaling were directly responsible for microtubule reorganization, we would expect to observe a spatially graded response of oocyte microtubules because sperm in the spermatheca generate an extracellular MSP gradient such that proximal oocytes are exposed to greater MSP levels than distal oocytes (Kosinski et al., 2005). To test this possibility, we analyzed CMEF values among oocytes within a time point using *lsd* (Fig. 2B). Significantly lower CMEF values were observed in proximal (−1, −2, −3) than in distal (−4, −5) oocytes, supporting the idea that microtubule reorganization is spatially graded over the proximal gonad arm (Figs. 2A and B).

MSP is sufficient for oocyte microtubule reorganization

These time course data are consistent with the hypothesis that MSP may be sufficient to signal microtubule reorganization. To test this possibility directly, we injected 200 nM purified MSP or a control buffer into the uterus of unmated females. After various recovery times (30, 60, or 120 min), we quantified oocyte microtubule organization (Figs. 2D and E). Females injected with MSP exhibited a decreased average CMEF value of 1.23 ± 0.30 ($n=15$) by 30 min following MSP injection compared to buffer-injected controls, which displayed an average CMEF value of 1.61 ± 0.42 ($n=60$). Oocytes located more distal from the uterine injection site (e.g., oocytes −2 and −3) tended to exhibit higher CMEF values than the most proximal oocyte. These results provide evidence that the MSP signal is sufficient to reorganize microtubules in proximal oocytes. These results further suggest that as the MSP signal diminishes, oocyte microtubules become cortically enriched.

MSP signaling affects the localization and dynamics of oocyte microtubules

Localization of microtubule plus and minus ends

During oogenesis, centrioles and centrosomes are lost in many organisms; and in *C. elegans*, they disappear prior to the late stages of oocyte differentiation. To further analyze the organization of microtubules in *C. elegans* oocytes, we examined the localization of CeGrip-1, a component of the γ-tubulin ring complex, which nucleates and anchors the minus ends of microtubules (Hannak et al., 2002), and thus approximates the localization of microtubule minus ends. In the absence of sperm, we observed an enrichment of CeGrip-1 at the cortex (Fig. 3A, arrowheads), which is not seen in the presence of sperm (Fig. 3B). Rather, CeGrip-1 is diffusely distributed throughout the cytoplasm in the presence of sperm (Fig. 3B; the nuclear staining appears to represent a nonspecific cross-reaction). This suggests that microtubule nucleation at the oocyte cortex is increased in the absence of

sperm. In addition, we investigated the localization of growing plus ends using an EBP-2::GFP fusion construct (Srayko et al., 2005). Single confocal images reveal that growing microtubule plus ends are enriched at the cortex in the absence of sperm (Fig. 3C). By contrast, growing plus ends are distributed throughout the cytoplasm in the presence of sperm (Fig. 3D). This result mimics the distribution of CeGrip-1, suggesting that there is an increase in both microtubule nucleation and growth at the cortex of oocytes in the absence of sperm.

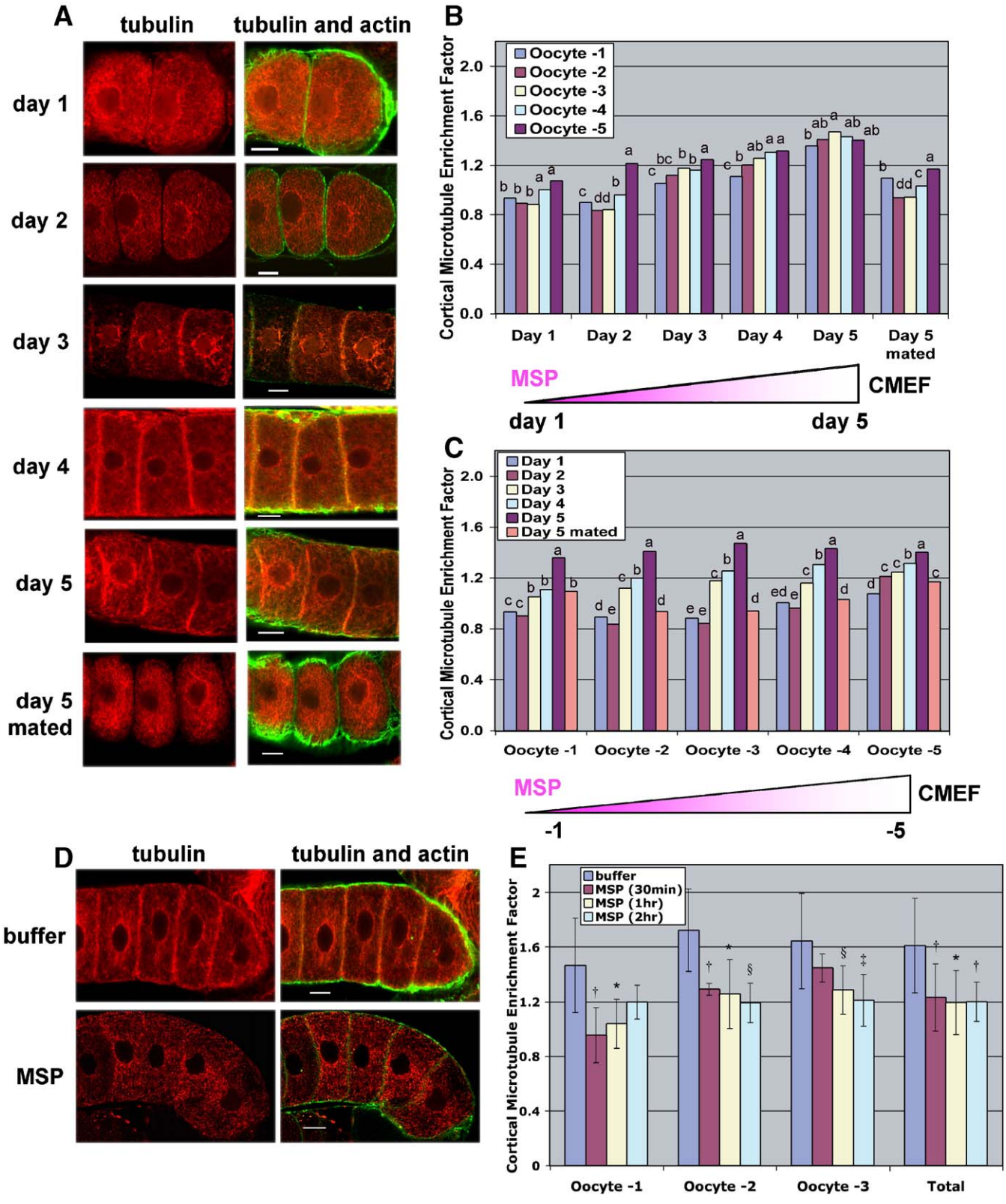

Dynamics of growing plus ends

To visualize the dynamic nature of microtubules in oocytes, we used spinning disk confocal microscopy to image the behavior of EBP-2::GFP, which marks growing microtubule plus ends (Srayko et al., 2005), in oocytes of living females and hermaphrodites. We visualized growing plus ends in 1-min stream acquisitions by tracking the movement of EBP-2::GFP foci that remained in the focal plane for 3–5 consecutive frames. We observed that growing plus ends appeared to move randomly throughout the oocyte cytoplasm in the presence of sperm (Fig. 3G; Supplementary Movie 1). In the absence of sperm, however, we observed a directional movement bias of growing microtubule plus ends at the oocyte cortex, in which they appeared to travel up and down along the proximal–distal cortex, or back and forth along the dorsal–ventral cortex (Fig. 3F; Supplementary Movie 2). Interestingly, in the cytoplasm of female oocytes, the plus ends appeared to move along tracks or bundles extending from the nucleus to the cortex (Fig. 3F, white arrows). Growing microtubule plus ends that contacted the nuclear envelope appeared to move more rapidly, similar to observations made in embryos by Srayko et al. (2005), who suggested this behavior is due to dynein motors localized at the cytoplasmic face of the nuclear envelope. We also noticed that the dissection protocol increased the rate of spontaneous maturation of the −1 oocyte, and that growing microtubule plus ends appeared to move randomly (Fig. 3F, asterisk) in these spontaneously maturing oocytes.

In order to quantify sperm-dependent differences in microtubule behavior, we examined the density, direction, and rate of movement of growing plus ends at multiple regions of the oocyte in the absence and presence of sperm, at the proximal–distal cortex, the dorsal–ventral cortex, the cytoplasm, and around the nuclear envelope. To compare the density of growing plus ends in EBP-2::GFP females and hermaphrodites, we measured the number of actively growing plus ends in a 36.4-μm^3 volume at various regions of the oocyte, focusing on strong staining foci within the focal plane. We observed that oocytes contained a higher density of growing plus ends in the absence of sperm at each region of the oocyte (Fig. 3E). In addition, the proximal and distal cortex exhibited the largest difference in plus-end density. In the absence of sperm, the number of growing plus ends at the proximal and distal cortex was 0.77±0.02 plus ends/μm^3 (n=30), whereas there was a significant decrease (almost three-fold, $p<0.0001$) in growing plus ends at the cortex in the presence of sperm (0.28±0.01 plus ends/μm^3, n=30) (Fig. 3E).

Directionality and rate of movement of growing plus ends

To assess the trajectories of growing plus ends in a quantitative manner, we tracked the movement of EBP-2::GFP foci that remained in the plane of focus over five consecutive frames (~1.5 s) for each region of the oocyte. We defined the distal to proximal axis as 0° and divided the oocyte medial plane into eight categories (A–H), each spanning a 45° interval (Fig. 3H). Growing plus ends were assigned to a category based on the direction vector of their movement. In the absence of sperm, growing plus ends displayed a directional movement bias at the proximal–distal and dorsal–ventral cortex of the oocyte (Figs. 3F–J, and Supplementary Fig. 1B). At the proximal and distal cortex in females, plus-end movement predominately fell into categories B, C, F, and G, corresponding to movement up and down along the cortex between oocytes (Figs. 3F and I). Likewise, at the dorsal or ventral cortex of the oocyte in females, moving plus-ends predominately fell into categories A, D, E, and H, corresponding to plus-end movement along the dorsal and ventral cortex of the oocyte (Figs. 3F and J). By contrast, in the presence of sperm growing plus ends exhibited uniformly distributed movement in each region of the oocyte (Figs. 3G–J, and Supplementary Fig. 1A). These data support our initial visual observations and suggest that MSP signaling affects both the spatial organization of microtubules and their directionality of movement.

To assess the rate of movement of growing microtubule plus ends at different regions of oocytes, we measured the distance EBP-2::GFP foci traversed over five consecutive frames (~1.5 s) in females and hermaphrodites (Fig. 3K). The rate of movement of EBP-2::GFP foci reflects microtubule growth as well as the physical translation of microtubules via motor action (Srayko et al., 2005). We observed that the rates of movement of growing plus ends were largely position independent in the absence and presence of sperm, with the exception of some plus ends that contacted the nuclear envelope (Fig. 3K and data not shown). We observed a significant ($p<0.001$) difference in the rate of plus-end movement between females and hermaphrodites (Fig. 3K). In females, plus ends move at a slightly slower rate (1.27±0.01 μm/s, n=400; Fig. 3K) compared to hermaphrodites (1.65±0.08 μm/s, n=400; Fig. 3K). The slower movement rate observed in females might be reflective of the

Fig. 2. MSP is sufficient to reorganize oocyte microtubules. (A) Single confocal images of hermaphrodite oocytes labeled with tubulin (red) and actin (green) during the time course. Day 4 hermaphrodites were mated with males and analyzed on day 5 (bottom panel). (B) Comparison of cortical microtubule enrichment over time (between 13 and 17 gonad arms were analyzed per time point). When MSP is present during the first few days of adulthood, the CMEF is low. As hermaphrodites age and MSP is depleted, the CMEF increases. The wedge depicting the MSP gradient is an estimate for illustrative purposes—see Kosinski et al. (2005) for measurements. The *lsd* method was used to compare the means of different oocytes at each time. Means with the same letter designation are not significantly different from one another within each individual day grouping (e.g., a=a, b=bc, and bc=c); whereas means with different letter designations are significantly different ($p<0.01$; e.g., b≠c, but bc=c and bc=b). Distal oocytes exhibit higher CMEF values than proximal oocytes. (C) Comparison of cortical microtubule enrichment by oocyte. The *lsd* method was used to compare means at different time points for each individual oocyte. For each oocyte, CMEF values are lower earlier in adulthood when extracellular MSP levels are higher. (D) Effect of MSP on oocyte microtubule reorganization. Females were injected with either 200 μM purified MSP or a control buffer. Single confocal images of oocytes are labeled with tubulin (red) and actin (green). Microtubules appear cortically enriched in buffer-injected females and reorganized in MSP-injected females. (E) Quantification of oocyte microtubule reorganization in MSP-injected females, which were allowed to recover for 30 min, 1 h, or 2 h after injection (t test between buffer-injected females and each MSP injection condition, *$p<0.0001$, §$p<0.001$, †$p<0.01$, ‡$p<0.05$, error bars represent SD). Scale bars: 10 μm.

overall increase in the density of growing plus ends observed in the absence of sperm (Fig. 3E).

FRAP analysis of oocyte microtubules

The data presented above suggest that MSP affects microtubule organization and dynamics in oocytes. To determine whether the exchange rate of free tubulin into microtubules is also affected by the presence of sperm, we conducted FRAP experiments in unmated and mated female oocytes expressing β-tubulin::GFP (Fig. 3L). We bleached a 74-μm^2 area within several regions of the oocyte and allowed recovery to occur over 2 min. We normalized the recovered-fluorescence intensity values to the whole-cell and background fluorescence intensities and calculated the recovery halftimes at each region (Table 1). Examination of the β-tubulin::GFP FRAP curves at the proximal and distal cortices indicated a significantly slower recovery in the absence of sperm (Fig. 3L), with a recovery halftime at the proximal–distal cortex of 14.06±3.90 s (n=19)

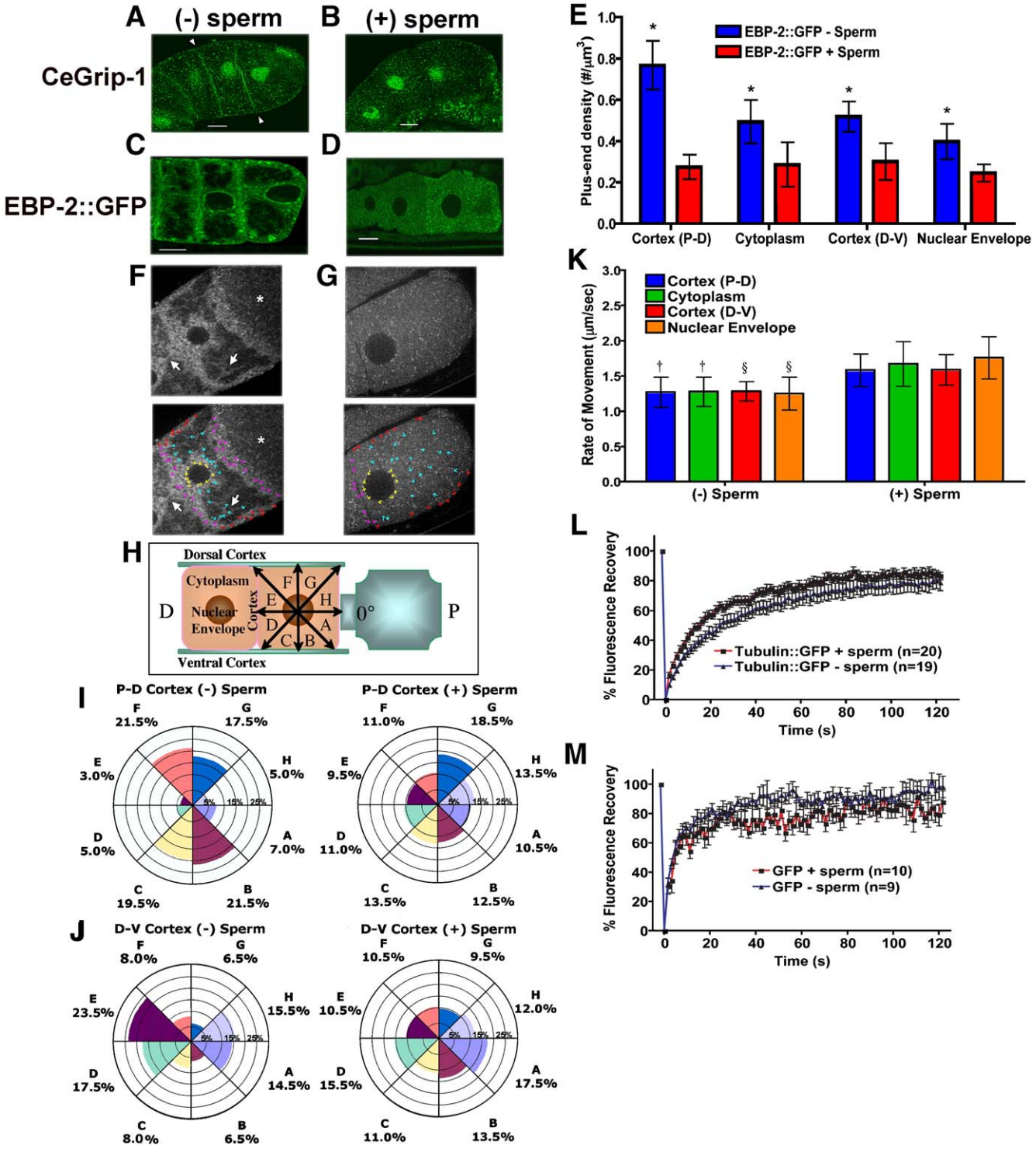

Table 1
FRAP halftimes (s)

Genotype	Sperm	Cytoplasm (*n*)	P-D Cortex (*n*)	D-V Cortex (*n*)
GFP [a]	+	3.57±1.78 (*n*=10)	3.43±1.62 (*n*=10)	2.89±0.92 (*n*=10)
GFP	−	3.28±1.63 (*n*=9)	3.81±1.11 (*n*=9)	2.92±0.66 (*n*=10)
Tubulin: :GFP [b]	+	9.78±4.94 (*n*=23)	9.55±3.97 (*n*=20)	8.29±4.77 (*n*=22)
Tubulin: :GFP	−	12.02±5.44 (*n*=18)	14.06±3.90 (*n*=19) [c]	13.74±4.45 (*n*=19) [c]

[a] Hermaphrodites were analyzed for the sperm (+) condition.
[b] Mated females were analyzed for the sperm (+) condition.
[c] *t* test between the presence and absence of sperm is significant ($p<0.001$).

in females ($p<0.001$; Table 1) compared to 9.55±3.97 s ($n=20$) in mated females ($p<0.001$; Table 1). These data suggest that free tubulin may be incorporated into microtubules slightly slower at a population level in the absence of sperm. The increased number of growing microtubule plus ends in females (Fig. 3E) may compete for free tubulin, thereby producing the longer halftime. As a control, we performed FRAP analysis on oocytes expressing cytoplasmic GFP in the germ line in the absence and presence of sperm (Fig. 3M). The initial fluorescence recovery curves tightly overlapped when we compared data from the cortex of females and hermaphrodites (Fig. 3M), and the halftimes at the cortex did not differ markedly (Table 1; $p>0.1$). These data indicate that the presence of sperm does not affect the diffusion rate of cytoplasmic GFP. Taken together, these analyses of microtubule dynamics suggest that changes in the cortical density of growing microtubule plus ends may represent a major factor in MSP-dependent microtubule reorganization.

Antagonistic Gα$_s$ and Gα$_{o/i}$ signaling pathways in the soma regulate oocyte microtubule reorganization

ceh-18, but not vab-1, affects microtubule reorganization

MSP promotes oocyte meiotic maturation by antagonizing two parallel negative regulatory circuits: an oocyte VAB-1, Eph/MSP receptor, pathway, and a somatic gonadal sheath cell pathway defined by the POU-homeoprotein, CEH-18 (Fig. 1A; Miller et al., 2003). To determine whether either of these pathways affect MSP-dependent oocyte microtubule reorganization, we examined oocytes from unmated and mated *vab-1 (null)* and *ceh-18(null)* mutant females (Figs. 4A–E). *vab-1 (dx31)* null mutants did not have an effect on microtubule reorganization either in the absence (CMEF=1.91±0.20, $n=15$; Figs. 4B and E) or presence (CMEF=0.97±0.18, $n=20$; Figs. 4A and E) of sperm. By contrast, *ceh-18(mg57)* null mutant females did not exhibit cortical microtubule enrichment in the absence of sperm (CMEF=1.03±0.12, $n=18$) (Figs. 4D and E), but contained evenly dispersed microtubules throughout the cytoplasm as in mated females (CMEF=0.92±0.14, $n=14$) (Figs. 4C and E). Likewise, oocytes in *vab-1(dx31);ceh-18(mg57)* mutant females exhibited reorganized microtubules (CMEF=0.99±0.12, $n=18$) (Fig. 4E). These results indicate that the *ceh-18* pathway inhibits microtubule reorganization in the absence of MSP, thereby suggesting a role for the gonadal sheath cells in regulating the organization of oocyte microtubules.

Gα$_s$ signaling promotes oocyte microtubule reorganization

A recent study suggested that the gonadal sheath cells regulate meiotic maturation via antagonistic Gα$_s$ and Gα$_{o/i}$ signaling pathways, which function in parallel to the VAB-1 Eph/MSP receptor pathway (Govindan et al., 2006). In this study, Gα$_s$ signaling was shown to be necessary to promote meiotic maturation and MAPK activation in oocytes in the presence of MSP (Govindan et al., 2006). In addition, Gα$_s$ signaling was shown to be sufficient for these responses in the absence of MSP. To test whether *gsa-1*, which encodes Gα$_s$, affects microtubule reorganization, we analyzed microtubules following *gsa-1(RNAi)* in a hermaphrodite background (Fig. 4G). We observed that oocyte microtubules were cortically enriched at the proximal and distal edges following *gsa-1 (RNAi)* in the presence of sperm (CMEF=1.73±0.30, $n=54$) (Figs. 4G and P) compared to the empty vector RNAi control (CMEF=0.80±0.19, $n=33$) (Figs. 4F and P), indicating that *gsa-1* is required for MSP-dependent microtubule reorganization. To determine whether *gsa-1* functions in the soma or the germ line to promote microtubule reorganization, we conducted RNAi analysis in an *rrf-1(null)* mutant background. *rrf-1*

Fig. 3. MSP affects the localization and dynamics of microtubules. (A and B) Single confocal images of a fixed unmated (A) and mated (B) *fog-2(q71)* female labeled with CeGrip-1 antibodies. CeGrip-1 is dispersed in a punctate fashion throughout the cytoplasm in the presence of sperm (B), but there is cortical enrichment (arrowheads) in the absence of sperm (A). The nuclear staining is likely due to cross-reactivity of the antibody. (C and D) Single confocal images of a live unmated female (C) and hermaphrodite (D) expressing EBP-2: :GFP. EBP-2: :GFP is enriched at the cortex in unmated females (C) but is dispersed in a punctate fashion throughout the cytoplasm in hermaphrodites (D). (E) Density of growing microtubule plus ends at different regions of the oocyte in females and hermaphrodites (*t* test between females and hermaphrodites, *$p<0.0001$, error bars represent SD). (F and G) Upper panels show spinning-disk confocal images of an EBP-2: :GFP unmated female (F) and hermaphrodite (G). Lower images are overlaid with multicolored arrows that correspond to the direction of plus-end movement at different regions of the oocyte (red=D-V cortex, purple=P-D cortex, blue=cytoplasm, and yellow=nuclear envelope). (F) The white arrows indicate tracks within the unmated female oocyte that growing plus ends predominantly move along. The white asterisk indicates an oocyte that has spontaneously matured in the absence of sperm. (H) Diagram showing the strategy for categorizing the directional movement of growing plus ends. In a clockwise manner from the proximal edge of the oocyte, categories were assigned in 45° intervals (labels from A–H), corresponding to the direction vector of plus-end movement. (I and J) Circular diagrams demonstrating the percentage of plus ends per 45° category at the P-D cortex (I) or the D-V cortex (J) of females and hermaphrodites, as indicated. The chi-square test was used to test the null hypothesis that microtubule plus ends exhibit uniform directional movement. The null hypothesis was rejected in females at the P-D and D-V cortices ($p<0.001$). (K) Rate of plus-end movement in females and hermaphrodites at different regions of the oocyte (*t* test between female and hermaphrodite, $^{\S}p<0.001$, $^{\dagger}p<0.01$, error bars represent SD). (L) FRAP curves of tubulin: :GFP in unmated and mated females. The fluorescence-recovery curves do not overlap at initial times, suggesting that tubulin: :GFP is incorporated from free pools slightly faster in the presence of sperm. (M) FRAP curves of germline-expressed GFP in females and hermaphrodites. The fluorescence-recovery curves tightly overlap at initial times, suggesting that there is no difference in the diffusion rate of free GFP in the absence and presence of sperm. Table 1 reports the halftimes for the FRAP analysis. Scale bars: 10 μm.

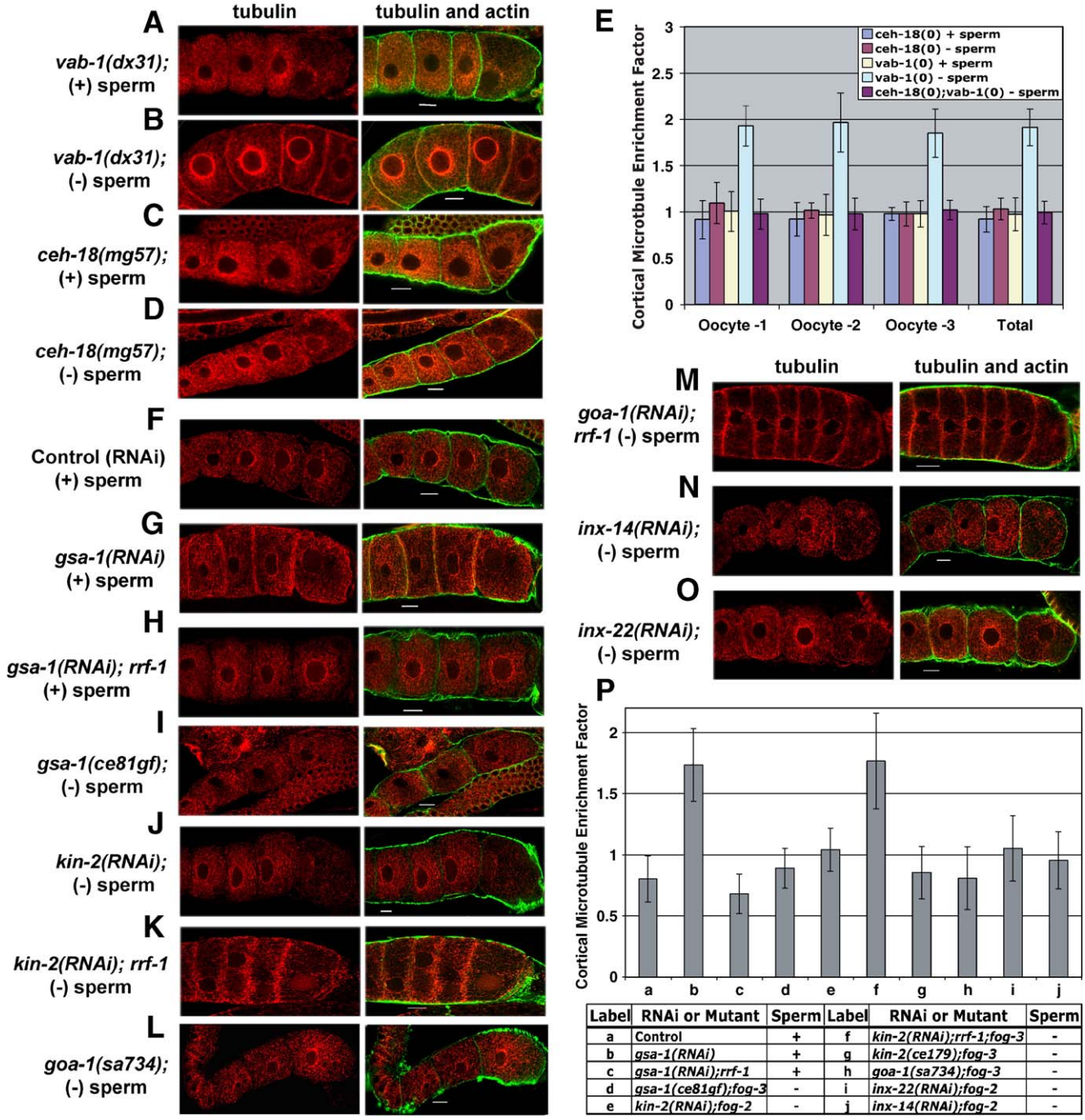

Label	RNAi or Mutant	Sperm	Label	RNAi or Mutant	Sperm
a	Control	+	f	*kin-2(RNAi);rrf-1;fog-3*	-
b	*gsa-1(RNAi)*	+	g	*kin-2(ce179);fog-3*	-
c	*gsa-1(RNAi);rrf-1*	+	h	*goa-1(sa734);fog-3*	-
d	*gsa-1(ce81gf);fog-3*	-	i	*inx-22(RNAi);fog-2*	-
e	*kin-2(RNAi);fog-2*	-	j	*inx-14(RNAi);fog-2*	-

Fig. 4. MSP signaling genes regulate oocyte microtubule reorganization. (A and B) Single confocal images of *vab-1(dx31)* mated (A) and unmated (B) females labeled with tubulin (red) and actin (green). Null mutations in *vab-1* have no effect on microtubule organization. (C and D) Single confocal images of *ceh-18(mg57)* mated (C) and unmated (D) females. Unmated females (D) do not exhibit cortical microtubule enrichment. (E) CMEF measurements in *ceh-18* and *vab-1* mutants in the absence and presence of sperm (error bars represent SD). (F–O) Single confocal images of dissected gonads from mutants or RNAi-treated animals labeled as indicated. (F) Hermaphrodites treated with empty-vector control RNAi. (G) Hermaphrodites treated with *gsa-1* RNAi. (H) *rrf-1(pk1417)* hermaphrodites treated with *gsa-1* RNAi. (I) *gsa-1(ce81gf)fog-3(q443)* unmated females. (J) Unmated *fog-2* females treated with *kin-2* RNAi. (K) Unmated *fog-3(q443)rrf-1(pk1417)* females treated with *kin-2* RNAi. (L) *goa-1(sa734)fog-3(q443)* unmated females. (M) *fog-3(q443)rrf-1(pk1417)* unmated females treated with *goa-1* RNAi. (N) Unmated *fog-2* females treated with *inx-14* RNAi. (O) Unmated *fog-2* females treated with *inx-22* RNAi. (P) CMEF measurements for the indicated genotypes (between 6 and 18 gonad arms were analyzed; error bars represent SD). Scale bars: 10 μm.

encodes an RNA-dependent RNA polymerase (RdP) that is required for the RNAi response in many somatic cells (Sijen et al., 2001) but is dispensable for germline RNAi, which employs the EGO-1 RdP (Smardon et al., 2000). Thus, an RNAi response in an *rrf-1(null)* background is indicative of a germline function, whereas an absence of a response suggests sufficiency of gene function in the soma. We observed that microtubules were not enriched at the proximal–distal cortex of oocytes

following *gsa-1(RNAi)* in an *rrf-1(null)* mutant background (CMEF = 0.68 ± 0.16, n = 27; Figs. 4H and P), suggesting that $G\alpha_s$ signaling in the soma is sufficient to promote microtubule reorganization in oocytes in the presence of MSP.

To test whether *gsa-1* activity is sufficient to promote microtubule reorganization in the absence of MSP, we examined two gain-of-function (gf) *gsa-1* alleles, *ce94*gf and *ce81*gf, which are predicted to stabilize the GTP-bound form of $G\alpha_s$ through G45R and R182C substitutions, respectively (Schade et al., 2005). In *gsa-1(ce81*gf*)* and *gsa-1(ce94*gf*)* females, we observed that oocyte microtubules were dispersed evenly throughout the cytoplasm (CMEF = 0.88 ± 0.16, n = 17; Figs. 4I and P; and data not shown), like in mated females. In canonical $G\alpha_s$ signaling, activated $G\alpha_s$ stimulates adenylyl cyclase resulting in production of cAMP, which binds the regulatory subunit of cAMP-dependent PKA thereby releasing the active catalytic subunit (Cabrera-Vera et al., 2003). Thus, we tested the involvement of *kin-2*, which encodes the regulatory subunit of cAMP-activated protein kinase, in regulating oocyte microtubule reorganization. We examined oocyte microtubules in *kin-2(ce179);fog-3(q443)* females or following *kin-2(RNAi)* in a *fog-2(q71)* female background (Figs. 4J and P, and data not shown). In both cases, we observed that oocyte microtubules were reorganized despite the absence of MSP (CMEF = 0.85 ± 0.22, n = 15, and CMEF = 1.04 ± 0.18, n = 39, respectively).

To determine whether *kin-2* functions in the germ line or soma to prevent microtubule reorganization in the absence of MSP, we tested the effect of *kin-2(RNAi)* in an *rrf-1(pk1417) fog-3(q443)* female background. We observed cortically enriched microtubules (CMEF = 1.76 ± 0.39, n = 30) (Figs. 4K and P), indicating that *kin-2* function is sufficient in the soma to prevent oocyte microtubule reorganization when MSP is absent. This observation is consistent with the finding that *kin-2* functions in the soma to prevent meiotic maturation in the absence of MSP (Govindan et al., 2006). The contribution of both $G\alpha_s$ and KIN-2 to microtubule reorganization in oocytes suggests that cAMP may also be involved in this regulation. To test this hypothesis, we soaked unmated *fog-2(q71)* females in an 8 mg/ml solution of dibutyryl-cAMP for 2 h. Although the effects were weak, variable, and required high levels of dibutyryl-cAMP, they were quantifiable in that the dibutyryl-cAMP-soaked females exhibited decreased CMEF values (CMEF = 1.24 ± 0.21, n = 33) compared to the buffer control (CMEF = 1.61 ± 0.34, n = 60; $p < 0.001$; data not shown). Thus, $G\alpha_s$ signaling in the soma, likely in the gonadal sheath cells, is necessary and sufficient to promote oocyte microtubule reorganization.

$G\alpha_{o/i}$ signaling inhibits oocyte microtubule reorganization in the absence of sperm

Recently, Govindan et al. (2006) provided evidence that *goa-1*, which encodes a $G\alpha_{o/i}$ protein, functions in the sheath cell control of meiotic maturation and MAPK activation in oocytes. Specifically, *goa-1* was shown to negatively regulate meiotic maturation and MAPK activation when MSP was absent, and *gsa-1* was shown to be epistatic to *goa-1*. To determine whether *goa-1* is a regulator of oocyte microtubule reorganization, we examined *goa-1(sa734)fog-3(q443)* females and observed evenly dispersed microtubules (CMEF = 0.81 ± 0.26, n = 24) (Figs. 4L and P). By contrast, cortically enriched microtubules were observed following *goa-1(RNAi)* in an *rrf-1(null)* female background (Fig. 4M). These data suggest that *goa-1* is required in the soma to prevent oocyte microtubule reorganization in the absence of the MSP signal.

Regulation of oocyte microtubule reorganization by $G\alpha_s$, $G\alpha_{o/i}$, and gap junctions

To investigate the relationship between *goa-1* and *gsa-1* in the regulation of oocyte microtubule reorganization, we performed *gsa-1(RNAi)* on *goa-1(sa734)* hermaphrodites and examined oocyte microtubules. Microtubules were cortically enriched at the proximal and distal cortical edges of oocytes (data not shown) consistent with the finding that *gsa-1* is required for oocyte microtubule reorganization in a hermaphrodite background (Fig. 4G). When we conducted *gsa-1(RNAi)* in a *goa-1(sa734)fog-3(q443)* female background, however, oocyte microtubules were reorganized (Supplementary Fig. 2A). It has been recently reported that *gsa-1(RNAi)* in a *goa-1 (sa734)* female background results in low meiotic maturation rates and an absence of detectable MAPK activation in oocytes (Govindan et al., 2006), a result we confirmed. Thus, microtubule reorganization might represent a separable element of the meiotic maturation process requiring different thresholds of signaling. Together, these data suggest the involvement of antagonistic $G\alpha_s$ and $G\alpha_{o/i}$ signaling in sheath cells in the regulation of microtubule reorganization in oocytes.

$G\alpha_s$ signaling appears to promote meiotic maturation in part by affecting the synthesis or stability of sheath/oocyte gap junctions (Govindan et al., 2006). The existence of gap-junctional communication between sheath cells and oocytes provides a potential mechanism for coordinating their behaviors (Hall et al., 1999). To determine whether gap-junctional communication between sheath cells and oocytes regulates oocyte microtubule reorganization, we used RNAi to inactivate *inx-14* and *inx-22*, which likely encode innexin components of the sheath/oocyte gap junctions (Govindan et al., 2006). When we conducted *inx-14(RNAi)* or *inx-22(RNAi)* in a *fog-2(q71)* female background, we observed oocytes that contained evenly dispersed microtubules (CMEF = 0.95 ± 0.23 (n = 15) and CMEF = 1.05 ± 0.27 (n = 18), respectively) (Figs. 4N–P). These data suggest that gap-junctional communication between sheath cells and oocytes prevents microtubule reorganization in the absence of MSP.

Germline regulators of oocyte microtubule reorganization

To identify oocyte regulators of microtubule reorganization, we conducted a candidate-gene screen, focusing on genes implicated in meiotic maturation control or microtubule regulation (summarized in Table 2; Supplementary Fig. 2). MSP-dependent MAPK activation and meiotic maturation require the downstream action of OMA-1 and OMA-2, two

Table 2
Screen for regulators of microtubule reorganization [a]

Gene	Description
I. Genes that promote microtubule reorganization in the presence of sperm	
gsa-1 [b]	Heterotrimeric $G_s\alpha$ protein subunit
oma-1/oma-2 [c]	Redundant TIS11 zinc finger proteins
II. Genes that prevent microtubule reorganization in the absence of sperm	
kin-2 [b]	cAMP-dependent protein kinase (regulatory subunit)
cgh-1 [b]	RNA DEAD-box helicase
ceh-18 [c]	POU-class homeobox transcription factor
wee-1.3 [d]	Wee1/Myt1 cdc2-inhibitory kinase
emo-1 [c]	Sec61pγ ortholog
ptc-1 [c]	Patched receptor
gpb-1 [d]	Heterotrimeric G_β protein subunit
goa-1 [b]	Heterotrimeric $G_{o/i}\alpha$ protein subunit
inx-14 [d]	Gap junction protein (innexin family)
inx-22 [d]	Gap junction protein (innexin family)
III. Microtubule regulators that had no effect on microtubule reorganization in the presence or absence of sperm	
cls-2 [d]	Microtubule tip-binding protein
dhc-1 [d]	Cytoplasmic dynein heavy chain
dnc-1 [d]	Dynactin
gip-1 [d]	Gamma-tubulin-binding protein
khc-1 [d]	Kinesin heavy chain
klc-1 [d]	Kinesin light chain
klp-7 [d]	Atypical kinesin-like motor protein
klp-13 [d]	Kinesin-like protein
klp-15 [d]	C-terminal motor kinesin
klp-16 [d]	Kinesin motor protein
klp-18 [d]	Kinesin-like protein
mbk-2 [d]	Yak1-related kinase protein member
mei-1 [d]	Catalytic subunit of katanin
mei-2 [d]	P80 targeting subunit of katanin
ndc-80 [d]	Member of HEC/Ndc80p family
nmy-2 [d]	Nonmuscle myosin II
ptl-1 [d]	Microtubule binding protein
ran-1 [d]	RAN GTPase
tac-1 [d]	Transforming acidic coiled-coil protein
tba-2 [d]	Alpha tubulin
tba-9 [d]	Alpha tubulin
zen-4 [d]	Kinesin-like protein
zyg-9 [d]	Microtubule-associated protein
C55A6.2 [d]	Tubulin-tyrosine-like ligase

[a] Between 30 and 40 gonad arms were analyzed by confocal microscopy.
[b] Both RNAi and mutants were used for phenotypic analysis.
[c] Mutants were used for phenotypic analysis.
[d] RNAi was used for phenotypic analysis.

TIS-11 zinc-finger proteins expressed in the germ line (Detwiler et al., 2001). When we examined microtubules in *oma-1 (zu405te33);oma-2(te51)* double mutant hermaphrodites, microtubules were enriched at the proximal and distal cortex (Table 2; Supplementary Fig. 2B). This observation indicates that OMA-1 and OMA-2 may function to promote microtubule reorganization directly, or indirectly, as a consequence of their requirement for promoting meiotic maturation. Analysis of genetic mutants in three negative regulators of meiotic maturation and MAPK activation in oocytes, *emo-1(oz1)* (Iwasaki et al., 1996), *ptc-1(ok122)* (Govindan et al., 2006), and *cgh-1(ok492)* (I. Y. and D. G., unpublished results), indicated that these mutants exhibit reorganized oocyte microtubules in a female genetic background (Supplementary Figs. 2C–E).

Recently, Burrows et al. (2006) demonstrated that the Myt1 homolog WEE-1.3 is required for the normal timing of NEBD during the meiotic maturation process in hermaphrodites and for proper meiotic spindle assembly. Consistent with the proposal that *wee-1.3* regulates oocyte microtubules (Burrows et al., 2006), we found that *wee-1.3(RNAi)* in a *fog-2(q71)* female background causes oocyte microtubule reorganization (Supplementary Fig. 2F). Burrows et al. (2006) reported that *wee-1.3 (RNAi)* in a female background is not sufficient to trigger NEBD (Burrows et al., 2006); however, under our RNAi conditions *wee-1.3(RNAi)* was sufficient to cause NEBD (data not shown), suggesting the microtubule effect could be downstream of *cdk-1* activation. Whereas *cdk-1(RNAi)* in a hermaphrodite background did not block oocyte microtubule reorganization (data not shown), it may be difficult to completely deplete CDK-1 from the germline using RNAi, as discussed previously (Boxem et al., 1999; Burrows et al., 2006).

To begin to address the mechanism of microtubule reorganization, we used RNAi to test whether known microtubule regulators, such as kinesin and dynein motors and microtubule-associated proteins (Table 2, section III), function to promote oocyte microtubule reorganization when sperm are present or, alternatively, whether they are needed for blocking reorganization in female backgrounds. We found that none of the tested microtubule regulators (Table 2, section III) affected oocyte microtubule reorganization, indicating that further work will be needed to determine the mechanism at the level of individual microtubules.

Oocyte microtubule reorganization does not require high levels of MAPK activation

MSP signaling triggers MAPK activation in oocytes (Miller et al., 2001). Because there is a general correlation between MAPK activation and oocyte microtubule reorganization: negative regulators of MAPK activation (e.g., *kin-2*, *inx-14*, *inx-22*, *ptc-1*, *cgh-1*, *goa-1*, *gpb-1*, *ceh-18*) block microtubule rearrangement in females, whereas positive regulators (e.g., *oma-1/2* and *gsa-1*) are required in hermaphrodites, we addressed the requirement for *mpk-1* MAPK. Because null mutations in *mpk-1* MAPK cause a sterile phenotype in which germ cells fail to progress through pachytene thereby disrupting oogenesis at an early stage (Church et al., 1995), we tested the involvement of *mpk-1* MAPK using three methods that reduce but not eliminate *mpk-1* activity: (1) the temperature-sensitive (ts) *mpk-1(ga111*ts*)* allele; (2) *mpk-1(RNAi)*; and (3) the chemical inhibitor U0126. One-day-old adult hermaphrodites were shifted to the restrictive temperature (25°C) for 12–16 h and their oocyte microtubules were analyzed by confocal microscopy. All gonad arms examined containing oocytes exhibited microtubule reorganization for both *mpk-1(ga111ts)* ($n=10$) and *mpk-1(RNAi)* ($n=8$). We also injected the gonads of young adult hermaphrodites with a 100-μM solution of the MEK1/2 inhibitor, U0126, as an additional approach for inhibiting MAPK activation. When we assessed the efficacy of the U0126 injections by staining dissected gonads with antibodies to the diphosphorylated, activated form of MPK-1

MAPK (MAPK-YT), we found that only 50% of the gonads exhibited observable MAPK-YT staining ($n=40$). In contrast, staining of U0126-injected gonads with anti-α-tubulin antibodies indicated that microtubules were reorganized in all proximal oocytes. Together these results suggest that MAPK activation may not be essential for MSP-dependent microtubule reorganization. This result is consistent with the observation, described above, that oocyte microtubules are reorganized following *gsa-1(RNAi)* in a *goa-1(sa734)fog-3(q443)* female background, despite the lack of observable MAPK activation in oocytes. The interpretation of these results has the major caveat that we cannot exclude the possibility that residual levels of activated MAPK may be available for promoting oocyte microtubule reorganization.

Discussion

MSP signaling reorganizes oocyte microtubules

In addition to nuclear changes presaging the final steps of meiotic chromosome segregation, the meiotic maturation process encompasses cytoplasmic alterations, collectively referred to as "cytoplasmic maturation," which include reorganization of cytoplasmic organelles, cytoskeletal remodeling, activation of signaling for ovulation, and cellular events important for fertilization and polarity establishment (reviewed by Greenstein and Lee, 2006; Voronina and Wessel, 2003; Yamamoto et al., 2006). The full extent of the cytoplasmic meiotic maturation program and its regulation is considerably less well understood than the control of meiotic cell cycle progression. In this report, we investigate changes in the oocyte microtubule cytoskeleton during early steps of the meiotic maturation process in *C. elegans*. We provide evidence that the sperm-derived meiotic maturation signal, MSP, triggers cytoplasmic microtubule reorganization in the oocyte prior to NEBD. When MSP is absent, as in females or older hermaphrodites, microtubules are enriched at the proximal and distal cortices of oocytes. In mated females or younger hermaphrodites, microtubules are dispersed evenly in a net-like fashion throughout the cytoplasm of proximal oocytes. We used a quantitative assay for oocyte microtubule reorganization to show that purified MSP is sufficient to direct this cytoskeletal remodeling. Using spinning disk confocal microscopy to assess microtubule dynamics in living animals, we found that the presence of MSP affects the localization and density of growing plus ends, as well as their directionality of movement. Overall, these studies reveal that a remarkable change in the microtubule cytoskeleton occurs in response to the MSP meiotic maturation hormone and that these changes occur prior to both NEBD and fertilization.

The microtubules changes we describe here, which we term "oocyte microtubule reorganization," are distinct from "oocyte cortical rearrangement," or the rounding-up of the oocyte just prior to ovulation, described by McCarter and Schedl (1999), in at least two significant ways. First, oocyte microtubule reorganization occurs prior to the onset of NEBD, whereas oocyte cortical rearrangement occurs after the onset of NEBD (McCarter et al., 1999). Second, oocyte cortical rearrangement is spatially restricted to the maturing −1 oocyte and occurs in the time window between the onset of NEBD and ovulation (3–5 min prior to ovulation). By contrast, proximal oocytes that receive the MSP signal undergo microtubule reorganization. The possibility that oocyte cortical rearrangement (McCarter et al., 1999) represents an actin-based process is consistent with static images of phalloidin- or anti-actin-stained fixed gonads and embryos (Strome, 1986), but real-time analysis will be needed to address this possibility fully. MSP signaling thus induces an early reorganization of the microtubule cytoskeleton, which might be followed by later changes in the actin cytoskeleton.

Microtubules play critical roles during oogenesis by controlling cell shape, protein trafficking, RNA localization, and cell polarity. Despite these essential functions, it is incompletely understood how meiotic or follicular signals regulate microtubule organization and function in oocytes. We used quantitative confocal microscopy and genetics to analyze the regulation of oocyte microtubule reorganization. Our analyses defined two groups of regulators: the first group promotes microtubule reorganization in the presence of MSP; and the second group prevents reorganization in the absence of MSP (Table 2). A null mutation in the POU-homeobox gene *ceh-18* leads to microtubule reorganization in a female genetic background in which MSP is absent. This finding, taken together with the observation that *ceh-18* is expressed in gonadal sheath cells but not oocytes, and is required for proper sheath cell differentiation and function (Greenstein et al., 1994; Rose et al., 1997), suggests a role for the gonadal sheath cells in controlling the microtubule cytoskeleton of the oocyte. Consistent with this idea, *goa-1*, which encodes a $G\alpha_{o/i}$ protein shown to inhibit meiotic maturation through its action in the soma (Govindan et al., 2006), is a negative regulator of oocyte microtubule reorganization. Further, we used the *rrf-1* genetic background, in which somatic cells are less sensitive to RNAi, to provide evidence that *goa-1* functions in the soma to prevent oocyte microtubule reorganization in the absence of sperm. To explore how sheath cell signaling might influence the localization and dynamics of microtubules within oocytes, we tested several known germline-expressed microtubule regulators (e.g., microtubule-associated proteins and motors) for their potential involvement using RNAi, but none of the tested microtubule regulators had an effect. Although it will take further work to uncover the mechanism by which the somatic gonad controls microtubule localization and dynamics in oocytes, signaling through sheath/oocyte gap junctions is likely to play an important role, as *inx-14(RNAi)* or *inx-22(RNAi)* cause microtubule reorganization in female genetic backgrounds. These findings mesh with prior TEM studies that indicated that sheath/oocyte gap junctions were rare or absent in *ceh-18* mutants (Rose et al., 1997; Hall et al., 1999). These observations raise the possibility that small molecules or ions transferred through these junctions might critically influence microtubule localization and dynamics.

MSP signaling stimulates the basal contraction of the proximal sheath cells (McCarter et al., 1999; Miller et al.,

2001). Several observations allow us to discount the possibility that the absence or presence of external mechanical pressure from sheath cell contractions represents a major factor regulating MSP-dependent oocyte microtubule reorganization. For example, *oma-1(zu40te33);oma-2(te51)* mutant hermaphrodites exhibit substantial sheath cell contractions (5.6±3.6 contractions/min; $n=14$; I.Y., D.G., unpublished results), but lack oocyte microtubule reorganization, whereas *ceh-18(mg57)* females exhibit low basal sheath cell contraction rates, but have reorganized oocyte microtubules.

What is the biological significance of MSP-dependent oocyte microtubule reorganization?

To address the potential function of oocyte microtubule reorganization, we attempted to determine the consequence of blocking the process. We found two situations in which oocyte microtubule reorganization was disrupted despite the presence of MSP: (1) *oma-1(zu40te33);oma-2(te51)* hermaphrodites; and (2) *gsa-1(RNAi)* hermaphrodites. Because meiotic maturation, ovulation, and fertilization do not occur in the *oma-1;oma-2* double mutant (Detwiler et al., 2001), we were unable to discern whether there is a detrimental consequence for the embryo. In a similar vein, meiotic maturation only occurs at a low rate following *gsa-1(RNAi)* (Govindan et al., 2006). The few fertilization events we observed following *gsa-1(RNAi)*, typically one per gonad arm, resulted in viable hermaphrodite offspring, perhaps suggesting a nonessential or modulatory role for oocyte microtubule reorganization. Nonetheless, several considerations affect the interpretation of this result. First, for technical reasons, we could not address whether microtubule reorganization can occur in the few maturing oocytes observed following *gsa-1(RNAi)*, similar to that seen in spontaneous meiotic maturation events in a female background. Second, we were unable to examine *gsa-1(null)* hermaphrodites owing to the fact that *gsa-1* is an essential gene (Korswagen et al., 1997), and thus the caveat that RNAi was used in this experiment should be considered. Genetic or experimental (i.e., RNAi) perturbations that specifically affect microtubule reorganization, but not other components of the meiotic maturation process, will be needed to address the question of biological significance more fully.

Although it is formally possible that MSP-dependent oocyte microtubule reorganization is nonessential, our bias is that this dramatic cytoskeletal transformation has functional importance for the worm, which we can as of yet, only guess. Nonetheless, here we hazard a few speculations. In the first model, we suggest that microtubule reorganization might facilitate the assembly of the meiotic spindle (Fig. 5A). Because MSP affects the localization and the directionality of movement of growing microtubule plus ends, these changes in microtubule dynamics may promote search and capture of meiotic chromatin after NEBD (see Fig. 5A and Supplementary Movie 3). Thus, MSP may "prime" microtubule dynamics for meiotic spindle assembly early in the process, so that the spindle can form rapidly upon NEBD. Because cortical microtubule enrichment, as assessed by CMEF measurements, depends on oocyte position and sperm availability (Figs. 2B and C), we asked whether the meiotic spindle assembles more rapidly at the young-adult stage (day 1) when sperm are abundant compared to later in adulthood (day 3) when sperm are limiting. We made tubulin::GFP movies using spinning disk confocal microscopy of day 1 ($n=5$) and day 3 ($n=3$) adults. The time from NEBD to assembly of a bipolar meiotic spindle was approximately the

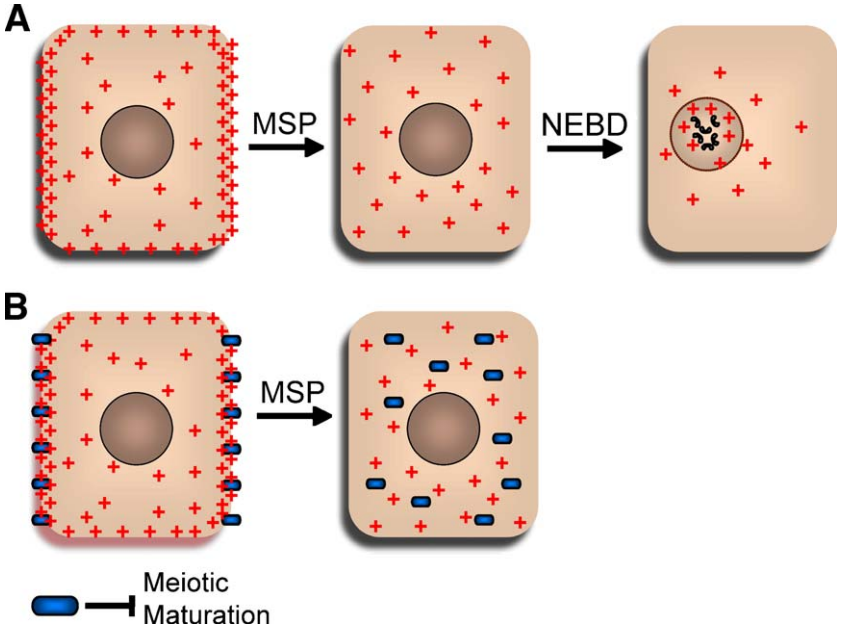

Fig. 5. Models for the biological significance of MSP-dependent oocyte microtubule reorganization. (A) Microtubule reorganization prepares the oocyte for meiotic spindle assembly upon NEBD. Changes in microtubule localization and dynamics (indicated by plus signs) in the presence of MSP facilitate search and capture of chromatin by microtubules. (B) Microtubule reorganization repatterns the oocyte cortex to facilitate the irreversible cell-cycle transition of meiotic maturation. Cortical reorganization may affect the trafficking of membrane proteins that inhibit meiotic maturation (depicted in blue).

same in both cases (9.86±3.48 vs. 11.0±2.73 min, respectively). Thus, sperm availability affects the frequency of meiotic maturation, but apparently not the timing of spindle assembly once maturation occurs. It remains a formal possibility, however, that oocyte microtubule reorganization may have a redundant role in influencing the timing of meiotic spindle assembly.

In a second, but not mutually exclusive model, cortical microtubule enrichment in the absence of MSP might facilitate trafficking of proteins needed to maintain meiotic diapause (Fig. 5B). For instance, meiotic arrest depends on the assembly of sheath/oocyte gap junctions and the function of the VAB-1 MSP/Eph receptor (Miller et al., 2003; Corrigan et al., 2005; Govindan et al., 2006). These regulators are likely to depend on microtubules for trafficking to the cortex (reviewed by Musch, 2004). By contrast, removal or depletion of negative regulators of meiotic maturation from the cortex upon microtubule reorganization might aid in flipping an "all or none" switch that drives the oocyte to meiotically mature once it reaches the most proximal position. Interestingly, we observed an asymmetry of cortical microtubule accumulation in the −1 oocyte in the absence of sperm in that microtubules were enriched at the distal but not the proximal cortex. Although the significance of this finding is unclear, we speculate that this asymmetry may be part of the mechanism by which this oocyte "knows" it is in the most proximal position and thus competent to undergo meiotic maturation upon receiving the MSP signal.

Microtubule reorganization in response to MSP signaling might also play a role in refashioning the cortex or plasma membrane domains for the later developmental events of fertilization or embryogenesis. At anaphase I, the DYRK-family kinase MBK-2 translocates from the cell cortex to intracellular puncta in a trafficking process that depends on CDK-1 and the anaphase-promoting complex (McNally and McNally, 2005; Stitzel et al., 2006). Although prior studies have not addressed whether microtubules play a key role in promoting MBK-2 redistribution, it is interesting that microtubules in the embryo are themselves a downstream target of MBK-2. MBK-2 phosphorylates the MEI-1 subunit of katanin, a dimeric microtubule-severing AAA-ATPase (Srayko et al., 2000), which marks it for ubiquitin-mediated degradation by a CUL-3/MEL-26 E3 ubiquitin ligase (Furukawa et al., 2003; Pintard et al., 2003). MEI-1 is required for assembly of anastral barrel-shaped female meiotic spindles (Clark-Maguire and Mains, 1994), and the inappropriate inclusion of MEI-1 into mitotic spindles is lethal because excessive shortening of astral microtubule arrays disrupts spindle positioning and the asymmetric partitioning of cell-fate determinants (Clandinin and Mains, 1993). The pioneering work of Mains and colleagues (1990) brought attention to the fact that meiotic and mitotic spindles form in a common cytoplasm, yet each utilizes different assembly mechanisms and mediates distinct functions, implying uniquely tailored regulatory modes. Our work here defines two classes of microtubule arrangements in oocytes: one associated with diapause; and the other associated with meiotic maturation. Both modes appear to represent active states with several genes required for their maintenance, suggesting complex regulation. We anticipate that the underlying mechanisms controlling cytoplasmic microtubule organization in this system may be relevant to the oocytes or epithelial cells of other organisms in which most microtubules are noncentrosomal.

Acknowledgments

We are grateful to Al Reynolds and Nicole Lobdell for generously sharing their spinning disk confocal microscope and providing training and assistance. We thank Anne Kenworthy and Jeffrey Shawn Goodwin for advice on the FRAP analysis. Sam Wells and Sean Schaffer provided helpful suggestions for optimizing live-cell imaging. Bob Barstead, Gary Moulder, Martin Srayko, Geraldine Seydoux, and the *Caenorhabditis* Genetic Center kindly provided strains. We thank Karen Oegema and Tony Hyman for their gift of the CeGrip-1 antibodies and Byeong Cha and Barth Grant for critical reading of the manuscript. J.E.H. would like to thank Mary Kosinski and Brandon Lute for their ideas and encouragement. This work was supported by NIH grants GM65115 and GM57173 (D.G.) and an NIH Training Grant 2T32HD007043-31 (J.E.H.).

Appendix A. Supplementary data

Supplementary data associated with this article can be found, in the online version, at doi:10.1016/j.ydbio.2006.07.013.

References

Albertson, D.G., Thomson, J.N., 1993. Segregation of holocentric chromosomes at meiosis in the nematode, *Caenorhabditis elegans*. Chromosom. Res. 1, 15–26.

Bottino, D., Mogilner, A., Roberts, T., Stewart, M., Oster, G., 2002. How nematode sperm crawl. J. Cell Sci. 115, 367–384.

Boxem, M., Srinivasan, D.G., van den Heuvel, S., 1999. The *Caenorhabditis elegans* gene *ncc*-1 encodes a cdc2-related kinase required for M phase in meiotic and mitotic cell divisions, but not for S phase. Development 126, 2227–2239.

Boyle, J.A., Ernst, S.G., 1989. Sea urchin oocytes possess elaborate cortical arrays of microfilaments, microtubules, and intermediate filaments. Dev. Biol. 134, 72–84.

Burrows, A.E., Sceurman, B.K., Kosinski, M.E., Richie, C.T., Sadler, P.L., Schumacher, J.M., Golden, A., 2006. The *C. elegans* Myt1 ortholog is required for the proper timing of oocyte maturation. Development 133, 697–709.

Cabrera-Vera, T.M., Vanhauwe, J., Thomas, T.O., Medkova, M., Preininger, A., Mazzoni, M.R., Hamm, H.E., 2003. Insights into G protein structure, function, and regulation. Endocr. Rev. 24, 765–781.

Carazo-Salas, R.E., Guarguaglini, G., Gruss, O.J., Segref, A., Karsenti, E., Mattaj, I.W., 1999. Generation of GTP-bound Ran by RCC1 is required for chromatin-induced mitotic spindle formation. Nature 400, 178–181.

Church, D.L., Guan, K.L., Lambie, E.J., 1995. Three genes of the MAP kinase cascade, *mek-2*, *mpk-1/sur-1 and let-60 ras*, are required for meiotic cell cycle progression in *Caenorhabditis elegans*. Development 121, 2525–2535.

Clandinin, T.R., Mains, P.E., 1993. Genetic studies of *mei-1* gene activity during the transition from meiosis to mitosis in *Caenorhabditis elegans*. Genetics 134, 199–210.

Clark-Maguire, S., Mains, P.E., 1994. Localization of the *mei-1* gene product of

Caenorhaditis elegans, a meiotic-specific spindle component. J. Cell Biol. 126, 199–209.

Corrigan, C., Subramanian, R., Miller, M.A., 2005. Eph and NMDA receptors control Ca2+/calmodulin-dependent protein kinase II activation during *C. elegans* oocyte meiotic maturation. Development 132, 5225–5237.

Detwiler, M.R., Reuben, M., Li, X., Rogers, E., Lin, R., 2001. Two zinc finger proteins, OMA-1 and OMA-2, are redundantly required for oocyte maturation in *C. elegans*. Dev. Cell 1, 187–199.

Furukawa, M., He, Y.J., Borchers, C., Xiong, Y., 2003. Targeting of protein ubiquitination by BTB-Cullin 3-Roc1 ubiquitin ligases. Nat. Cell Biol. 5, 1001–1007.

Govindan, J.A., Cheng, H., Harris, J.E., Yamamoto, I., Greenstein, D., 2006. $G\alpha_{o/i}$ and $G\alpha_s$ signaling function in parallel with the MSP/Eph receptor to control meiotic diapause in *C. elegans*. Curr. Biol. 16, 1–12.

Greenstein, D., Lee, L.A., 2006. Oocyte-to-embryo transition: kinase cabal plots regime change. Curr. Biol. 16, R93–R95.

Greenstein, D., Hird, S., Plasterk, R.H., Andachi, Y., Kohara, Y., Wang, B., Finney, M., Ruvkun, G., 1994. Targeted mutations in the *Caenorhabditis elegans* POU homeo box gene *ceh-18* cause defects in oocyte cell cycle arrest, gonad migration, and epidermal differentiation. Genes Dev. 8, 1935–1948.

Hall, D.H., Winfrey, V.P., Blaeuer, G., Hoffman, L.H., Furuta, T., Rose, K.L., Hobert, O., Greenstein, D., 1999. Ultrastructural features of the adult hermaphrodite gonad of *Caenorhabditis elegans*: relations between the germ line and soma. Dev. Biol. 212, 101–123.

Hannak, E., Oegema, K., Kirkham, M., Gonczy, P., Habermann, B., Hyman, A.A., 2002. The kinetically dominant assembly pathway for centrosomal asters in *Caenorhabditis elegans* is gamma-tubulin dependent. J. Cell Biol. 157, 591–602.

Hassold, T., Hunt, P., 2001. To err (meiotically) is human: the genesis of human aneuploidy. Nat. Rev. Genet. 2, 280–291.

Heald, R., Tournebize, R., Blank, T., Sandaltzopoulos, R., Becker, P., Hyman, A., Karsenti, E., 1996. Self-organization of microtubules into bipolar spindles around artificial chromosomes in *Xenopus* egg extracts. Nature 382, 420–425.

Hodges, C.A., Ilagan, A., Jennings, D., Keri, R., Nilson, J., Hunt, P.A., 2002. Experimental evidence that changes in oocyte growth influence meiotic chromosome segregation. Hum. Reprod. 17, 1171–1180.

Italiano Jr., J.E., Roberts, T.M., Stewart, M., Fontana, C.A., 1996. Reconstitution in vitro of the motile apparatus from the amoeboid sperm of Ascaris shows that filament assembly and bundling move membranes. Cell 84, 105–114.

Iwasaki, K., McCarter, J., Francis, R., Schedl, T., 1996. *emo-1*, a *Caenorhabditis elegans* Sec61p gamma homologue, is required for oocyte development and ovulation. J. Cell Biol. 134, 699–714.

Kalab, P., Pu, R.T., Dasso, M., 1999. The ran GTPase regulates mitotic spindle assembly. Curr. Biol. 9, 481–484.

Kamath, R.S., Ahringer, J., 2003. Genome-wide RNAi screening in *Caenorhabditis elegans*. Methods 30, 313–321.

Khodjakov, A., Cole, R.W., Oakley, B.R., Rieder, C.L., 2000. Centrosome-independent mitotic spindle formation in vertebrates. Curr. Biol. 10, 59–67.

Kilmartin, J.V., Wright, B., Milstein, C., 1982. Rat monoclonal antitubulin antibodies derived by using a new nonsecreting rat cell line. J. Cell Biol. 93, 576–582.

Korswagen, H.C., Park, J.H., Ohshima, Y., Plasterk, R.H., 1997. An activating mutation in a *Caenorhabditis elegans* Gs protein induces neural degeneration. Genes Dev. 11, 1493–1503.

Kosinski, M., McDonald, K., Schwartz, J., Yamamoto, I., Greenstein, D., 2005. *C. elegans* sperm bud vesicles to deliver a meiotic maturation signal to distant oocytes. Development 132, 3357–3369.

Mains, P.E., Kemphues, K.J., Sprunger, S.A., Sulston, I.A., Wood, W.B., 1990. Mutations affecting the meiotic and mitotic divisions of the early *Caenorhabditis elegans* embryo. Genetics 126, 593–605.

Matthies, H.J., McDonald, H.B., Goldstein, L.S., Theurkauf, W.E., 1996. Anastral meiotic spindle morphogenesis: role of the non-claret disjunctional kinesin-like protein. J. Cell Biol. 134, 455–464.

McCarter, J., Bartlett, B., Dang, T., Schedl, T., 1999. On the control of oocyte meiotic maturation and ovulation in *Caenorhabditis elegans*. Dev. Biol. 205, 111–128.

McNally, K.L., McNally, F.J., 2005. Fertilization initiates the transition from anaphase I to metaphase II during female meiosis in *C. elegans*. Dev. Biol. 282, 218–230.

Miller, M.A., Nguyen, V.Q., Lee, M.H., Kosinski, M., Schedl, T., Caprioli, R.M., Greenstein, D., 2001. A sperm cytoskeletal protein that signals oocyte meiotic maturation and ovulation. Science 291, 2144–2147.

Miller, M.A., Ruest, P.J., Kosinski, M., Hanks, S.K., Greenstein, D., 2003. An Eph receptor sperm-sensing control mechanism for oocyte meiotic maturation in *Caenorhabditis elegans*. Genes Dev. 17, 187–200.

Musch, A., 2004. Microtubule organization and function in epithelial cells. Traffic 5, 1–9.

Ohba, T., Nakamura, M., Nishitani, H., Nishimoto, T., 1999. Self-organization of microtubule asters induced in *Xenopus* egg extracts by GTP-bound Ran. Science 284, 1356–1358.

Page, S.L., Hawley, R.S., 2004. The genetics and molecular biology of the synaptonemal complex. Annu. Rev. Cell Dev. Biol. 20, 525–558.

Pintard, L., Willis, J.H., Willems, A., Johnson, J.L., Srayko, M., Kurz, T., Glaser, S., Mains, P.E., Tyers, M., Bowerman, B., Peter, M., 2003. The BTB protein MEL-26 is a substrate-specific adaptor of the CUL-3 ubiquitin-ligase. Nature 425, 311–316.

Praitis, V., Casey, E., Collar, D., Austin, J., 2001. Creation of low-copy integrated transgenic lines in *Caenorhabditis elegans*. Genetics 157, 1217–1226.

Rose, K.L., Winfrey, V.P., Hoffman, L.H., Hall, D.H., Furuta, T., Greenstein, D., 1997. The POU gene *ceh-18* promotes gonadal sheath cell differentiation and function required for meiotic maturation and ovulation in *Caenorhabditis elegans*. Dev. Biol. 192, 59–77.

Sampath, S.C., Ohi, R., Leismann, O., Salic, A., Pozniakovski, A., Funabiki, H., 2004. The chromosomal passenger complex is required for chromatin-induced microtubule stabilization and spindle assembly. Cell 118, 187–202.

Schade, M.A., Reynolds, N.K., Dollins, C.M., Miller, K.G., 2005. Mutations that rescue the paralysis of *Caenorhabditis elegans ric-8* (synembryn) mutants activate the G alpha(s) pathway and define a third major branch of the synaptic signaling network. Genetics 169, 631–649.

Schatten, G., 1994. The centrosome and its mode of inheritance: the reduction of the centrosome during gametogenesis and its restoration during fertilization. Dev. Biol. 165, 299–335.

Sijen, T., Fleenor, J., Simmer, F., Thijssen, K.L., Parrish, S., Timmons, L., Plasterk, R.H., Fire, A., 2001. On the role of RNA amplification in dsRNA-triggered gene silencing. Cell 107, 465–476.

Skold, H.N., Komma, D.J., Endow, S.A., 2005. Assembly pathway of the anastral *Drosophila* oocyte meiosis I spindle. J. Cell Sci. 118, 1745–1755.

Smardon, A., Spoerke, J.M., Stacey, S.C., Klein, M.E., Mackin, N., Maine, E.M., 2000. EGO-1 is related to RNA-directed RNA polymerase and functions in germ-line development and RNA interference in *C. elegans*. Curr. Biol. 10, 169–178.

Srayko, M., Buster, D.W., Bazirgan, O.A., McNally, F.J., Mains, P.E., 2000. MEI-1/MEI-2 katanin-like microtubule severing activity is required for *Caenorhabditis elegans* meiosis. Genes Dev. 14, 1072–1084.

Srayko, M., Kaya, A., Stamford, J., Hyman, A.A., 2005. Identification and characterization of factors required for microtubule growth and nucleation in the early *C. elegans* embryo. Dev. Cell 9, 223–236.

Stitzel, M.L., Pellettieri, J., Seydoux, G., 2006. The *C. elegans* DYRK kinase MBK-2 marks oocyte proteins for degradation in response to meiotic maturation. Curr. Biol. 16, 56–62.

Strome, S., 1986. Fluorescence visualization of the distribution of microfilaments in gonads and early embryos of the nematode *Caenorhabditis elegans*. J. Cell Biol. 103, 2241–2252.

Szollosi, D., Calarco, P., Donahue, R.P., 1972. Absence of centrioles in the first and second meiotic spindles of mouse oocytes. J. Cell Sci. 11, 521–541.

Varmark, H., 2004. Functional role of centrosomes in spindle assembly and organization. J. Cell Biochem. 91, 904–914.

Voronina, E., Wessel, G.M., 2003. The regulation of oocyte maturation. Curr. Top Dev. Biol. 58, 53–110.

Walczak, C.E., Vernos, I., Mitchison, T.J., Karsenti, E., Heald, R., 1998. A model for the proposed roles of different microtubule-based motor proteins in establishing spindle bipolarity. Curr. Biol. 8, 903–913.

Ward, S., Carrel, J.S., 1979. Fertilization and sperm competition in the nematode *Caenorhabditis elegans*. Dev. Biol. 73, 304–321.

Westermann, S., Weber, K., 2003. Post-translational modifications regulate microtubule function. Nat. Rev., Mol. Cell Biol. 4, 938–947.

Wilde, A., Zheng, Y., 1999. Stimulation of microtubule aster formation and spindle assembly by the small GTPase Ran. Science 284, 1359–1362.

Yamamoto, I., Kosinski, M.E., Greenstein, D., 2006. Start me up: cell signaling and the journey from oocyte to embryo in *C. elegans*. Dev. Dyn. 235, 571–585.